Interferometric Synthetic Aperture Radar (InSAR): Its Past, Present and Future

by
Zhong Lu, Ohig Kwoun, and Russell Rykhus

Introduction

Very simply, interferometric synthetic aperture radar (InSAR) involves the use of two or more synthetic aperture radar (SAR) images of the same area to extract landscape topography and its deformation patterns. A SAR system transmits electromagnetic waves at a wavelength that can range from a few millimeters to tens of centimeters and therefore can operate during day and night under all-weather conditions. Using SAR processing technique (Curlander and McDonough, 1991), both the intensity and phase of the reflected (or backscattered) radar signal of each ground resolution element (a few meters to tens of meters) can be calculated in the form of a complex-valued SAR image that represents the reflectivity of the ground surface. The amplitude or intensity of the SAR image is determined primarily by terrain slope, surface roughness, and dielectric constants, whereas the phase of the SAR image is determined primarily by the distance between the satellite antenna and the ground targets. InSAR imaging utilizes the interaction of electromagnetic waves, referred to as interference, to measure precise distances between the satellite antenna and ground resolution elements to derive landscape topography and its subtle change in elevation.

InSAR Past

The launch of the ERS-1 satellite in 1991 significantly promoted the development of InSAR techniques and applications. InSAR-related research in the 1990s can be grouped into three categories: deformation mapping, DEM generation, and landscape characterization. Initial applications of InSAR included the following,

Imaging earthquake displacement

InSAR was first applied to map the ground surface displacement caused by the 1992 Landers earthquake (Massonnet and Feigl, 1998). Using a pair of SAR images, one before the earthquake and the other after the earthquake, early research focused on mapping the co-seismic deformation with InSAR. Surface displacement data are extraordinarily useful for understanding slip distribution and rupture dynamics during earthquakes, and InSAR has made an indispensable contribution to seismology by providing earthquake location, fault geometry and rupture dynamics from the measured co-seismic deformation field. In the late 1990s, studies using InSAR to map ground surface deformation immediately after an earthquake (i.e., post-seismic deformation) yielded important clues to infer the properties of the Earth's crust and upper mantle.

Mapping ground surface deformation during volcanic eruptions

Early studies used SAR data acquired before and after a volcanic eruption to image the co-eruptive deformation. Surface deformation data from InSAR can provide essential information about magma dynamics. In the late 1990s, InSAR was used to map the deformation of volcanoes during quiescent periods. InSAR-derived surface deformation patterns shed important insights into the structure, plumbing, and state of restless volcanoes, and can be the first sign of increasing levels of volcanic activity, preceding swarms of earthquakes or other precursors that signal impending intrusions or eruptions (Lu, 2007) (Figure 1).

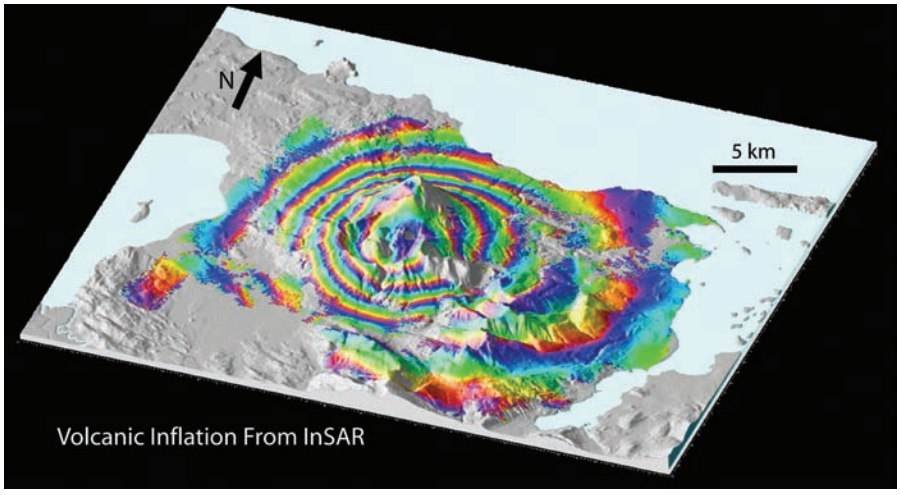

Figure 1. InSAR image shows six concentric fringes that represent about 17 cm of inflation centered on the southwest flank of Peulik, Alaska. Each fringe (full color cycle) represents 2.83 cm of change between the ground and the satellite. The volcano inflated aseismically from October 1996 to September 1998, a period that included an intense earthquake swarm that started in May 1998 and was located over 30 km northwest of Peulik Volcano.

continued on page 219

How InSAR Works

InSAR is formed by combining, or "interfering" radar signals from two spatially or temporally separated antennas. The spatial separation of the two antennas is called the baseline. The two antennas may be mounted on a single platform for simultaneous interferometry, which is the usual implementation for aircraft and spaceborne systems such as the Topographic SAR (TOPSAR) and the Shuttle Radar Topography Mission (SRTM) systems that were created for generating high-resolution, high-precision digital elevation models (DEMs) over large regions. Alternatively, InSAR can be created by using a single antenna on an airborne or spaceborne platform in nearly identical repeating flight orbits for repeat-pass interferometry (Massonnet and Feigl, 1998). In the latter case, even though the antennas do not illuminate a given area at the same time, the two sets of signals recorded during the two passes will be highly correlated if the scattering properties of the ground surface remain undisturbed between viewings. In this configuration, InSAR is capable of measuring ground-surface deformation with centimeter-to-subcentimeter precision at a spatial resolution of tens-of-meters over a large region. This is the typical implementation for spaceborne sensors such as:

1. U.S. SEASAT (operated June to October, 1978, L-band, wavelength λ = 25.0 cm),
2. European Remote-sensing Satellite (ERS-1) (operated 1991-2000, C-band, λ = 5.66 cm),
3. Japanese Earth Resources Satellite (JERS-1) (operated 1992-1998, L-band, λ = 23.5 cm),
4. Shuttle Imaging Radar-C (SIR-C) (operated April to October 1994, X-, C-, and L-band, λ = 3.1 cm, 5.66 cm, and 24.0 cm, respectively),
5. European Remote-sensing Satellite (ERS-2) (operating 1995-present, C-band, λ = 5.66 cm),
6. Canadian Radar Satellite (Radarsat-1) (operating 1995-present, C-band, λ = 5.66 cm),
7. European Environmental Satellite (Envisat) (operating 2002-present, C-band, λ = 5.63 cm), and
8. Japanese Advanced Land Observing Satellite (ALOS) (operating 2006-present, L-band, λ = 23.6 cm).

An InSAR image (also called an interferogram) is created by co-registering two SAR images and calculating the difference between their corresponding phase values on a pixel-by-pixel basis. The phase change (or range distance difference) in the original interferogram is caused mainly by five effects: (1) differences in the satellite orbits when the two SAR images were acquired, (2) landscape topography, (3) ground deformation, (4) atmospheric propagation delays, and (5) systematic and environmental noises. Knowledge of a satellite's position and attitude is required to remove the effect caused by the differences in the satellite orbits of the two passes. The topographic effects in the interferogram can be removed by producing a synthetic interferogram created from an accurate DEM and the knowledge of InSAR imaging geometry. The synthetic interferogram is then subtracted from the interferogram to be studied (Massonnet and Feigl, 1998). Alternatively, the topographic contribution can be removed through the use of a different interferogram of the same area. These procedures will remove the topography effect from InSAR images, and the component of ground deformation along the satellite's look direction can potentially be measured with a precision of centimeter or sub-centimeter for C-band sensors, and a few centimeters for L-band sensors. Because of problematic tropospheric propagation delay and ionospheric disturbance, repeat observations are critical to confidently interpret small geophysical signals related to movements of the Earth's surface. If the two SAR images are acquired simultaneously (i.e., single-pass InSAR), or the deformation during the SAR acquisition time is negligible, or can be modeled and removed, then the InSAR image can be used to derive a DEM (Lu et al., 2003). The single-pass InSAR is the fundamental building block for the generation of the SRTM DEM.

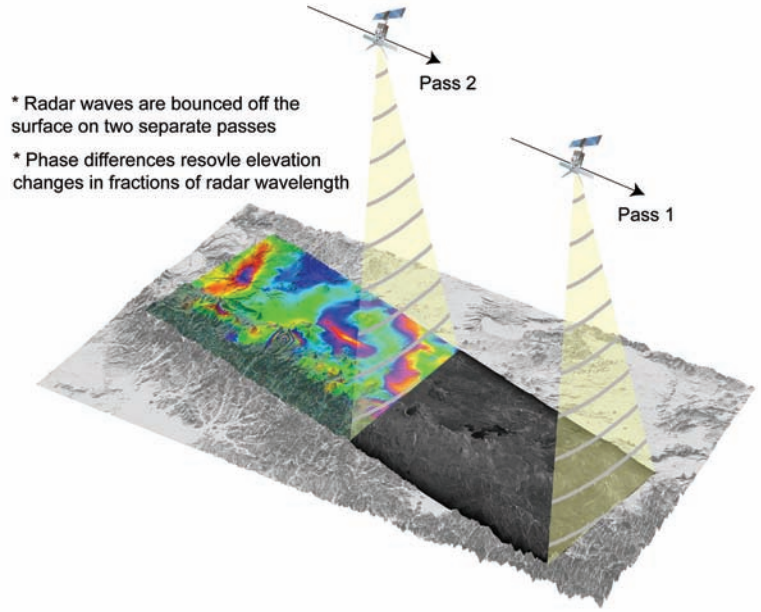

Illustration of how InSAR works (image courtesy of Charles Wicks/USGS).

continued from page 217

Mapping of land surface deformation associated with fluid withdrawal

Surface subsidence and uplift that were related to extraction and injection of fluids in groundwater aquifers and petroleum reservoirs can be seen in InSAR images. InSAR-based surface deformation mapping can provide fundamental data on reservoir/aquifer properties and processes, and improve the ability to assess and mitigate adverse consequences. InSAR capability was also demonstrated for mapping the slow movement of landslides, providing a new tool for landslide monitoring.

Recording the movement of glaciers

InSAR was successfully applied to record the movement of glaciers and ice fields, and significantly advanced the studies of glacier and ice flows and ice-sheet mass balance. By regularly imaging ice sheets over the Arctic, Antarctic, and Greenland, InSAR has contributed to building an unprecedented series of snapshots that document the short-term evolution of the ice sheet, aiding in the understanding of their impact on sea level change and global warming.

Mapping of water-level changes over wetlands

InSAR (particularly at longer wavelengths) was found to be an effective tool in the accurate measurement of water-level changes in river valleys and wetlands. Calibrated by in-situ measurements, the InSAR-derived water-level changes within wetlands will allow precise estimation of volumetric changes in water storage which can improve hydrological modeling predictions and enhance the assessment of future flood events over wetlands.

Use of InSAR to construct DEMs

InSAR was applied to construct DEMs over areas where the photogrammetric approach to DEM generation was hindered by inclement weather conditions. For example, repeat-pass InSAR was used to generate ice surface topography that determined the magnitude and direction of the gravitational force that drives ice flow and ice dynamics. In addition, volcano surface topography measurements from before and after an eruption were used to estimate the volume of extruded material. There are many sources of error in DEM construction from repeat-pass InSAR images: inaccurate determination of the InSAR baseline, atmospheric delay anomalies, and possible surface deformation due to tectonic, volcanic, or other loading sources over the time interval spanned by repeat-pass interferograms, etc. To generate a high-quality DEM from repeat-pass InSAR images, these errors must be corrected (Lu *et al.*, 2003).

The study of landscape characterization and changes

InSAR images and their associated products have proved useful for mapping flood extents, fire scars, land cover types, changes in soil moisture content, etc. For example, multiple SAR images can be used to map the progression of fire and to estimate fire severity. InSAR products that characterize the changes in SAR backscattering return (both intensity and phase signal) are indispensable for precise mapping of fire scar extents and severities (Figure 2).

continued on page 220

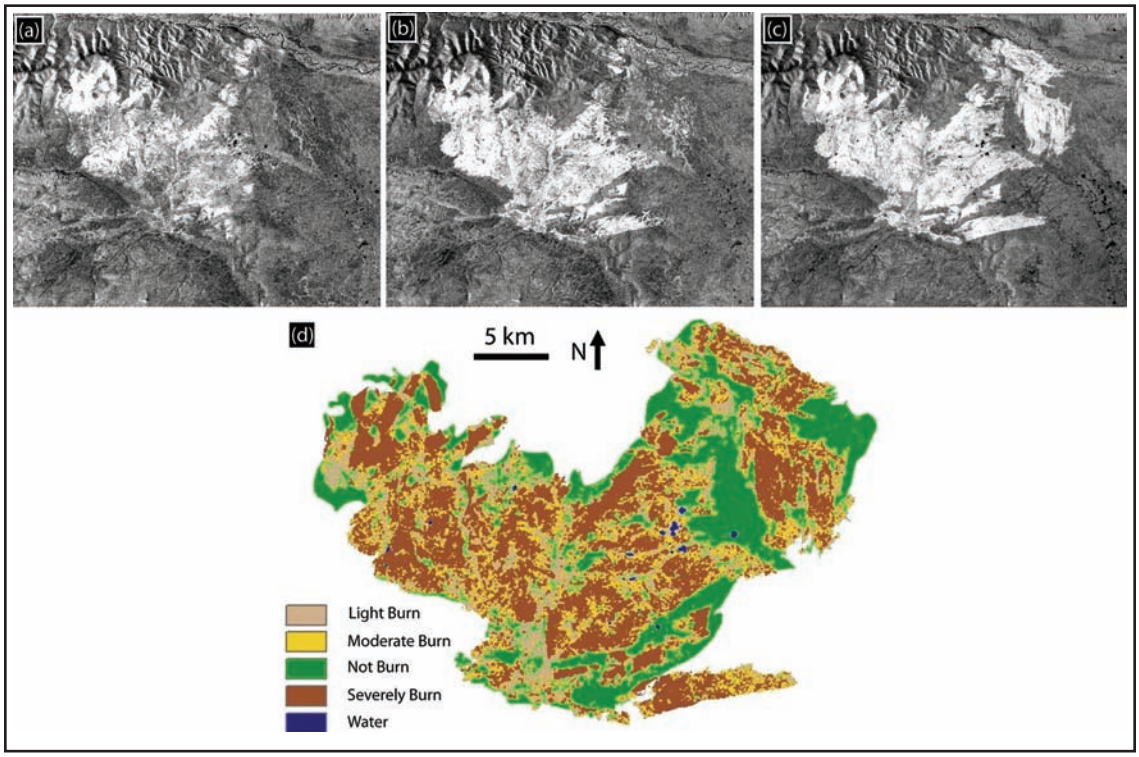

Figure 2. Radarsat-1 SAR intensity images over Yukon River Basin, Alaska acquired on a) August 17, 2003, b) September 10, 2003, and c) October 4, 2003. These SAR images show the procession of a fire that started in July of 2003. The derived fire severity map is shown in Figure 2d.

continued from page 219

InSAR Present

Deformation mapping with InSAR has advanced from the interpretation of a few InSAR image pairs to the analysis of multi-temporal, time-series InSAR images. The ultimate goal of the time-series analysis has been to reduce artifacts due to atmospheric delay anomalies, orbit errors, and loss of coherence measurements in order to improve the accuracy of deformation measurements. Stacking and least-squares inversion approaches, which take into account covariance characteristics of data distribution, have been applied to multi-temporal InSAR images to reduce atmospheric delay anomalies and improve temporal sampling in order to reveal transient, dynamic deformation patterns.

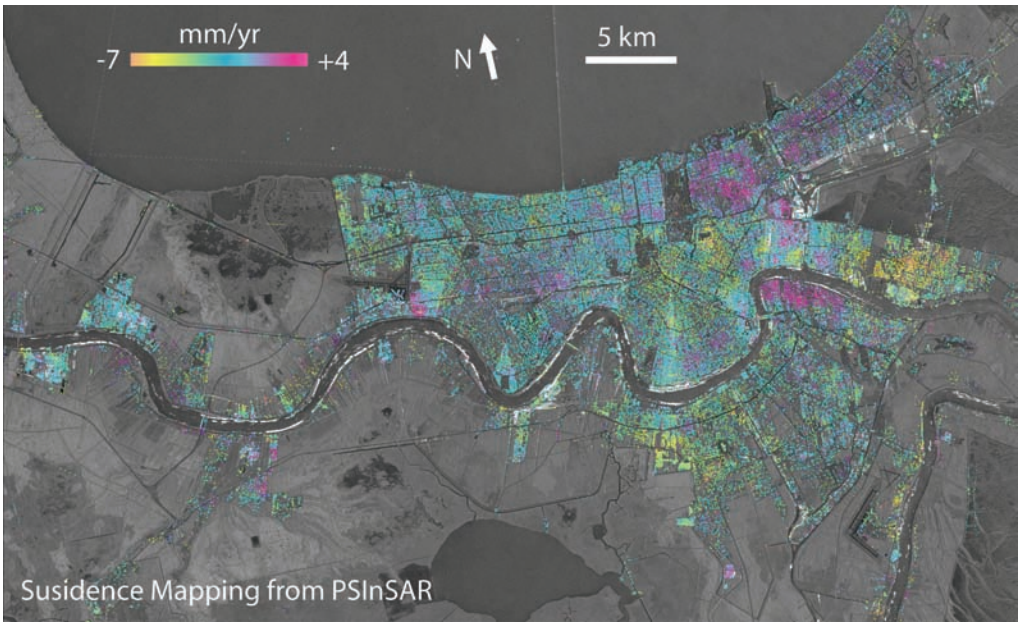

Figure 3. Average deformation image of New Orleans, southeastern Louisiana during 1992-1998, derived from multiple temporal InSAR images based on PSInSAR technique.

Persistent Scatterer (PS) InSAR (PSInSAR) represents the most significant advancement in InSAR research. PSInSAR uses unique characteristics of atmospheric delay anomalies and the distinctive backscattering of certain ground targets (called PS) to improve the accuracy of conventional InSAR deformation measurements from 10-20 mm to 2-3 mm (Ferretti et al., 2001). The SAR backscattering signal of a PS target has broadband spectra in the frequency domain, implying that the radar phase of this kind of scatterer correlates over much longer temporal intervals and over much larger baseline separations than other scatterers. As a result, if the backscattering return of a pixel is dominated by PS(s), this pixel will always be coherent over long time intervals. At PS pixels, the difficulty of decorrelation in conventional InSAR can therefore be overcome. In addition, the atmospheric contribution is rather smooth spatially and is independent over time. At PS pixels, the atmospheric contribution to the backscattered signal can be identified and removed from the data using a multi-interferogram approach. Therefore, the ultimate goal of PSInSAR processing is to separate the different contributions (surface deformation, atmospheric delay anomaly, DEM error, orbit error, and decorrelation noise) by means of least-squares estimations and iterations, taking into account the spatio-temporal distribution and the correlation between the PS samples. After removing errors due to the atmospheric anomaly, orbit error, and DEM error, deformation histories at PS points can be appreciated at millimeter accuracy (Figure 3). PSInSAR has been successfully applied to monitor landslides, urban subsidence, fault movement, and volcanic deformation.

In the meantime, applications of InSAR have made many ground-breaking discoveries in Earth science. For example, in earthquake study, InSAR has played an increasingly important role in mapping triggered slip, which occurs during an earthquake on a fault or faults not involved in the main shock ¬¬and is therefore extremely difficult to measure with conventional technology. InSAR is ideally suited to detect triggered slip because of its high spatial resolution, high measurement precision, and large areal coverage. In addition, InSAR can identify blind faults from the surface deformation patterns. Furthermore, InSAR has great potential to monitor interseismic deformation. Combined with seismology and other geophysical and geodetic measurements, InSAR can be expected to aid many breakthroughs in understanding the entire phase of the earthquake cycle (Wright, 2002).

InSAR Future

The next few years will witness more exciting technical and scientific breakthroughs in many aspects of InSAR. First, longer wavelength SAR images (such as L-band PALSAR onboard the ALOS) will be available that will enable InSAR deformation mapping at global scales where C-band InSAR can be plagued by loss of coherent signal because of vegetation. Second, fully-polarized SAR sensors (ALOS, Radarsat-2, TerraSAR-X, TanDEM-X, etc) will allow better characterization of vegetation structure and ground features. The combination of polarimetric and interferometric analysis (called Pol-InSAR) will offer a new capability for landscape mapping and deformation monitoring (Cloude and Papathanassiou, 1998). Pol-InSAR will enable optimization procedures that maximize the interferometric coherence and target decomposition approaches to the separation of radar backscattering returns from the canopy top, from the bulk volume of the vegetation, and from the ground surface. The difference in interferometric phase measurement then leads to the difference in height between the physical scatterers that possess these mechanisms. Accordingly, future Pol-InSAR instruments will enable significant advances in many fields of application: 1) land cover mapping and wetland mapping, particularly over regions where weather conditions hinder optical remote sensing; 2) inferring soil moisture with a horizontal resolution (several meters) that is not attainable otherwise; 3) mapping forest height and biomass with the generation of "bare-earth" DEMs; 4) monitoring ship traffic on the oceans, and much more.

A third breakthrough is ScanSAR, an advanced SAR imaging technique achieved by periodically switching the antenna look angle into neighboring subswaths in the range direction in order to increase the size of accessible range swath. ScanSAR will be equipped with InSAR capability to enhance spatial coverage of

conventional InSAR for large-scale deformation measurement and to improve temporal sampling of InSAR deformation images (Guarnieri and Rocca, 1999). Fourth, the atmospheric delays that hamper InSAR accuracy will be lessened by routinely estimating water-vapor content using a high-resolution weather model, continuous global positioning system (CGPS) network, or other satellite sensors such as the Moderate Resolution Imaging Spectroradiometer (MODIS), Advanced Spaceborne Thermal Emission and Reflection Radiometer (ASTER), and European Medium Resolution Imaging Spectrometer (MERIS) to improve InSAR deformation measurements (Foster et al., 2006). Fifth, advances in multi-temporal, multi-dimensional data-mining techniques (such as PSInSAR) will continue to improve deformation measurement, which will enable the mapping of time-variant ground surface deformation caused by many natural and man-made hazards.

Finally, automated SAR and InSAR processing systems will be more widely available, which will improve SAR/InSAR processing throughput and lay the foundation for routine monitoring of natural hazards and natural resources. Because more satellite radar sensors and radar satellite constellations become available in the next decade, the automated SAR/InSAR processing system is of paramount importance for near-real-time decision support.

Conclusion

InSAR is one of the fastest growing fields in Earth science and remote sensing. The precise land surface topography and their time-transient variability provided by InSAR systems will accelerate development of predictive models that can anticipate the behavior of many natural hazards such as volcanic eruptions, earthquakes, landslides, and others. In addition, InSAR will provide tools to better characterize the contribution of ground water, surface water, soil moisture, and snow to the global fresh water budget, and the role of glaciers and ice sheets in sea level rise and global warming. Furthermore, InSAR will offer the capability of imaging the three-dimensional structure of vegetation on a global scale for improved characterization and management of Earth's resources. With more and more operational SAR sensors available for rapid data acquisitions, armed with state-of-the-art information technologies such as data-mining and grid computation, InSAR will continue to address and provide solutions to many scientific questions related to natural hazard monitoring and natural resource management.

Acknowledgments

ERS-1/-2 and Radarsat-1 SAR images are copyrighted European Space Agency (ESA) and Canadian Space Agency (CSA), respectively, and were provided by the Alaska Satellite Facility (ASF) and ESA. This work was supported by funding from the NASA, the USGS Land Remote Sensing Program, and the USGS Volcano Hazards Program. Technical reviews by B. Wylie and C. Wicks are greatly appreciated. We thank C. Wicks for providing the figure illustrating how InSAR works.

References

Cloude S., and K. Papathanassiou, 1998. Polarimetric SAR interferometry, *IEEE Trans. Geosci. Remote Sensing*, 36, 1551-1565.

Curlander, J., and R. McDonough, 1991. *Synthetic aperture radar systems and signal processing*, New York: John Wiley & Sons.

Ferretti, A., C. Prati, and F. Rocca, 2001. Permanent scatterers in SAR interferometry, *IEEE Trans. Geosci. Remote Sensing*, 39, 8-20.

Foster, J., and others, 2006. Mitigating atmospheric noise for InSAR using a high resolution weather model, *Geophy. Res. Lett.*, 33, L16304, doi:10.1029/2006GL026781.

Guarnieri, A.M., and F. Rocca, 1999. Combination of Low- and High-Resolution SAR Images for Differential Interferometry, *IEEE Trans. Geosci. Remote Sensing*, 37, 2035-2049.

Lu, Z., E. Fielding, M. Patrick, and C. Trautwein, 2003. Estimating lava volume by precision combination of multiple baseline spaceborne and airborne interferometric synthetic aperture radar: the 1997 eruption of Okmok volcano, Alaska, *IEEE Trans. Geosci. Remote Sensing*, 41, 1428-1436.

Lu, Z., 2007. InSAR Imaging of Volcanic Deformation Over Cloud-prone Areas—Aleutian Islands, *Photogrammetric Engineering & Remote Sensing*, 245-257.

Massonnet, D., and K. Feigl, 1998. Radar interferometry and its application to changes in the Earth's surface, *Rev. Geophys.*, 36, 441-500.

Wright, T., 2002. Remote monitoring of the earthquake cycle using satellite radar interferometry, *Phil. Trans. R. Soc. Lond.*, 360, 2873-2888.

Authors

Zhong Lu
U.S. Geological Survey (USGS), Earth Resources Observation & Science (EROS) Center and David A Johnston Cascades Volcano Observatory, 1300 SE Cardinal Court, Vancouver, WA 98683-9589
phone: (360) 993 8911; email: lu@usgs.gov

Ohig Kwoun
Science Applications International Corporation (SAIC), Contractor to USGS EROS Center, 47914 252nd Street, Sioux Falls, SD 57198
phone: (605) 594 6153; email: okwoun@usgs.gov

Russell Rykhus
Science Applications International Corporation (SAIC), Contractor to USGS EROS Center, 47914 252nd Street, Sioux Falls, SD 57198
phone: (605) 594 6121; email: rykhus@usgs.gov